RSC Advances

PAPER

View Article Online
View Journal | View Issue

Cite this: *RSC Adv.*, 2025, **15**, 10501

Bromate removal in water through electrochemical reduction using Magnéli phase titanium oxide electrode†

Lun Guo, [a] David E. Williams, [bg] Lev Bromberg[c] and Lokesh P. Padhye [*adef]

Received 11th February 2025
Accepted 30th March 2025

DOI: 10.1039/d5ra01013f

rsc.li/rsc-advances

This study demonstrates the effective electrochemical degradation of bromate, achieving over 95% removal, using both sheet electrodes and reactive membranes fabricated from Magnéli phase titanium oxide (Ti_nO_{2n-1}, n = 4–10). Increasing the applied voltage and electrolyte concentration, as well as decreasing the pH, significantly enhanced bromate reduction efficiency. Experimental results suggest that both direct and indirect pathways contribute to the overall degradation process. The impact of coexisting ions was also evaluated. At 1 mM, their inhibitory effect was negligible, whereas, at 10 mM, the inhibition became pronounced in the order SO_4^{2-} > CO_3^{2-} > Cl^- ≈ NO_3^- ≈ NO_2^- > ClO_4^-. When applied to secondary effluent wastewater, this electrochemical approach achieved 70% degradation of bromate within six hours. Moreover, the Magnéli phase titanium oxide electrodes exhibited excellent stability and reusability, highlighting their potential for real-world water and wastewater treatment applications.

Introduction

Bromate (BrO_3^-) is classified as a "possible human" or "Group 2B" carcinogen by the International Agency for Research on Cancer (IARC). The maximum allowable bromate level in drinking water set by the United States Environmental Protection Agency (US EPA) is 10 μg L^{-1}. The formation of bromate in drinking water is commonly associated with disinfection using ozone.[1] Drinking water concentrations have been found to be up to 15 times higher than the regulation of 10 μg L^{-1}.[2] The optimization of ozonation operation conditions, such as lowering pH and controlling the ozone dose, can minimize the formation of bromate ions. However, such measures can also lead to a decrease in hydroxyl radical generation and, consequently, reduced treatment efficiency, greater formation of HOBr/brominated by-products, and lower degradation of contaminants.[3]

The addition of ammonia can also inhibit bromate formation during the ozonation process; however, it can only reduce the generation of bromate by 50%. Moreover, this approach is only feasible for water with 50–150 μg L^{-1} of bromide.[4] Therefore, post-treatment for bromate removal may be necessary if its formation cannot be avoided.

In the past decades, there have been a number of new technologies developed for bromate remediation, which include physical adsorption,[5] biological remediation,[6] catalytic reduction,[7,8] photochemical reduction,[9,10] and membrane separation.[11] Electrochemical reduction processes (ERPs) have also been investigated. The standard electrode potentials of bromate and HOBr are 1.48 V and 1.34 V *vs.* SHE, respectively, which indicate the possibility of electrochemical reduction of bromate in water.[12] The reduction process of bromate to bromide involves 6 electrons. The bromate reduction can be summarized as follows:[13]

$$BrO_3^- + 5H^+ + 4e^- \leftrightarrow HOBr + 2H_2O \quad (1)$$

$$HOBr + H^+ + 2e^- \leftrightarrow Br^- + H_2O \quad (2)$$

Reaction (1) is a complex, multi-step process, with deduced intermediate species $HBrO_2$ and $BrO_2^{\cdot}$; on Pt electrodes in acid solution, the intermediate species are autocatalytic for the reaction.[14] A redox-mediator autocatalytic cycle through the comproportionation reaction of bromate and product bromide to produce intermediate bromine can also be significant.[15]

[a]*Department of Civil & Environmental Engineering, The University of Auckland, Auckland, 1142, New Zealand*

[b]*School of Chemical Sciences, University of Auckland, Bldg. 302, 23 Symonds St, Auckland 1010, New Zealand*

[c]*Department of Chemical Engineering, Massachusetts Institute of Technology, Cambridge, MA 02139, USA*

[d]*Center for Clean Water Technology, Stony Brook University, Stony Brook, NY 11794, USA. E-mail: lokesh.padhye@stonybrook.edu*

[e]*School of Marine and Atmospheric Sciences, Stony Brook University, Stony Brook, NY 11794, USA*

[f]*Department of Civil Engineering, Stony Brook University, Stony Brook, NY 11794, USA*

[g]*MacDiarmid Institute for Advanced Materials and Nanotechnology, Wellington 6140, New Zealand*

† Electronic supplementary information (ESI) available. See DOI: https://doi.org/10.1039/d5ra01013f

Several electrode materials have been proposed as the cathode for the purpose of bromate reduction, such as metal electrodes,[14,16] bimetallic Pd/In, metal/metal oxide-carbon composites,[17–22] conductive polymers,[23,24] and boron-doped diamond (BDD).[25] However, there are research gaps in terms of understanding the stability/long-term reactivity and cost-effectiveness of these electrodes. For example, the electrocatalytic reduction of bromate by tungsten oxide (WO_3) has been observed.[26] However, the stability of the WO_3 electrode is an issue as it can be electrochemically reduced at −0.22 V *vs.* SCE.[26] Boron-doped diamond electrodes (BDD) can effectively degrade bromate ions, but BDD electrodes are synthesized by chemical vapor deposition, and the cost for production can be as high as $7125 per m^2.[27] It is necessary to find an alternative stable material that can perform bromate removal rapidly and cost-effectively.

Magnéli phase (MP) titanium oxide (Ti_nO_{2n-1}, $n = 4$ to 10) materials have been increasingly applied as fuel cell supports, battery electrodes, and in other applications because of their unique chemical, electrical, and magnetic properties.[28] These materials have the advantages of strong corrosion resistance, high mechanical strength, and excellent electrochemical stability under both anodic and cathodic polarization.[29] These attributes make MP titanium oxide materials promising for utilization as electrodes for oxidation and reduction of water contaminants. A number of studies have shown that MP titanium oxide anodes produce adsorbed "active oxygen" hydroxyl radicals, as shown in the following equation:[30]

$$MO_x + H_2O \rightarrow MO_x(^{\bullet}OH) + H^+ + e^- \quad (3)$$

The hydroxyl radicals are effective in the oxidation and removal of a wide range of recalcitrant organic and inorganic compounds.[28,29,31–33] The Ti_4O_7 anode exhibits a comparable oxygen evolution potential and comes with a deployment cost that is 60–70% lower than that of the BDD anode.[34] Other studies have shown that MP titanium oxide can be used as a cathode catalyst, facilitating the kinetics of oxygen reduction.[35,36]

In addition, the material can be fabricated into reactive membranes (REMs) with tailored porosities and various shapes that can be used on an industrial scale for water and wastewater treatment. The REMs can provide longer residence time and larger active surface area, which is beneficial for the degradation of contaminants.[33] Like the other REMs, MP titanium oxide REM can suffer from membrane fouling, but the foulant can be cleaned by polarity/flow reversal without undesired damage to the membrane.[37,38] The low cost of production and maintenance of MP titanium oxide also makes it economically feasible for use at an industrial scale.[39]

To date, no study has shown the reduction of bromate by MP titanium oxide in a continuous flow system with a commercially available electrochemical reactive membrane. In this study, the reduction of bromate on an MP titanium oxide sheet electrode is explored, and a larger-scale study of bromate electroreduction on an MP titanium oxide flow-through membrane is presented.

Materials and methods

Reagents and materials

Potassium bromate ($KBrO_3$), sodium perchlorate ($NaClO_4$), sodium chloride (NaCl), sodium nitrate ($NaNO_3$), sodium nitrite ($NaNO_2$), sodium carbonate (Na_2CO_3), sodium sulfate (Na_2SO_4), potassium dihydrogen phosphate (KH_2PO_4), and tertiary butanol (>99.9%) were purchased from Sigma-Aldrich. All chemicals were used without further purification. The synthetic solutions used in this study were prepared with ultrapure MQ water ($\rho = 18.2$ MΩ cm).

Magnéli phase titanium oxide sheet electrode, reactive membrane, and reactor setup

The MP titanium oxide sheet electrode and MP titanium oxide cylindrical industrial reactive membrane (IREM) were purchased from Ti-Dynamics Ltd, China. A customized membrane flow-through reactor was designed and made in-house at the University of Auckland. The reactor (0.18 m diameter, 0.48 m height) was made of acrylic tube (Cambrian Plastic, NZ). The diameter of the cylindrical membrane was 60 mm, with a porosity of 35% and a pore size of around 20 μm. The cylindrical counter electrode was made of stainless steel mesh with a diameter of 65 mm. See Fig. 1 for details of the configuration.

Analytical methods

MP titanium oxide materials were characterized by X-ray diffraction (XRD, Ultima IV, Rigaku) using CuKα radiation, and scans were collected at a 0.02° step size with 2θ range from 10 to 80°. Bromate and bromide were analyzed using Ion Chromatography (Dionex ICS-2100, Dionex IonPac™ AS19 Column). Dilution was applied when preparing the samples for IC.

Experiment procedures

Batch experiment with sheet electrode. A traditional three-electrode cell was used. 10 ml of a solution containing

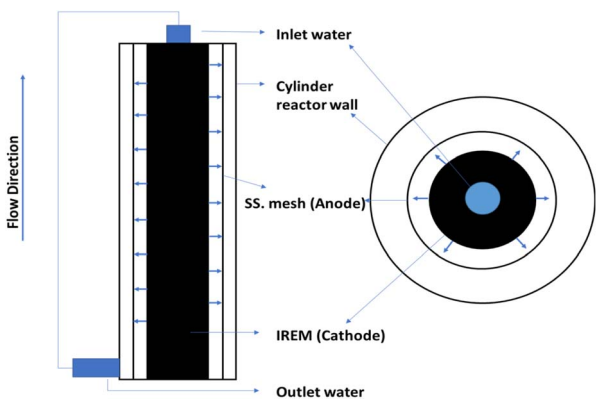

Fig. 1 Reactor setup. The solution containing bromate ions was fed into the reactor at the top inlet, and the permeate solution was collected/re-fed to the reactor at the bottom.

bromate with supporting electrolyte (100 mM KH_2PO_4, pH = 7.3) was added in each experiment. Samples were taken every 3 min for the first 15 min. If needed, one more sample was taken at 30 min. Each sample contained 0.05 ml of solution and was diluted to 0.5 ml for further analysis. All experiments were carried out at room temperature (~25 °C) in an open atmosphere, and the solution was well mixed with a magnetic stir bar at a setting of 100 rpm. MP titanium oxide sheet (~1 cm^2) was used as the cathode, and a similar size of stainless-steel mesh was used as the anode. All potentials were measured relative to the Ag/AgCl reference electrode and controlled with a potentiostat (Interface 1010E, Gamry).

All experiments with the sheet electrode were under conditions of the cathodic potential of −1.5 V, pH = 7.3, initial bromate concentration of 1 mM, and 100 mM electrolyte (KH_2PO_4) unless otherwise stated. The selection of −1.5 V was based on two key considerations. First, to ensure experimental consistency, the membrane electrode was initially tested at a cell potential of 3.25 V, which resulted in a cathodic potential of approximately −1.44 to −1.5 V. To maintain comparable conditions between the sheet electrode and the membrane electrode, −1.5 V was chosen. Second, preliminary tests with the sheet electrode showed that the highest bromate removal efficiency was achieved at this cathodic potential, making it the most effective choice for the study.

The degradation efficiency (DE) was calculated by using the following equation:

$$\mathrm{DE} = \frac{C_0 - C_t}{C_0} \tag{4}$$

where C_t and C_0 were the concentrations of bromate measured at time t and time 0. The degradation efficiency was fitted with a pseudo-first-order kinetic equation as shown below:

$$\ln\left(\frac{C_t}{C_0}\right) = -k_{obs}t \tag{5}$$

where k_{obs} is the kinetic pseudo-first-order rate constant (min^{-1}).

Flow-through experiment with IREM. 3 L of bromate solution was added to the reactor chamber. Before applying a potential to the IREM, the pump was switched on to circulate the feed and permeate solutions for 10–20 minutes, ensuring steady-state flow within the IREM. After the potentials were applied, samples were taken from the reactor outlet at a 20-minute time interval. Voltage was provided with a DC power supply (MP-3840, POWERTECH). The effect of cell voltage, pH, initial bromate concentration, and electrolyte concentration was determined. Experiments were under conditions of cell potential of 3.25 V, pH = 6.89, initial bromate concentration of 1 mM, and 100 mM electrolyte ($NaClO_4$) unless otherwise stated.

An experiment using real-world secondary effluent wastewater was performed with the flow-through reactor. The secondary effluent sample was collected from a wastewater treatment plant in Auckland, New Zealand, and used without further treatment. Bromate was added to the wastewater sample at a concentration of 1 mM before the experiment. The cell potential was set to 3.25 V. The reaction time was 6 h at a flow rate of 1711 liter m^{-2} h^{-1}.

Current efficiency (CE) was calculated as:

$$\mathrm{CE} = \frac{nFV(C_0 - C_f)}{It} \times 100 \tag{6}$$

where $n = 6$ is the electron number for the complete reduction of bromate to bromide, F denotes the Faraday constant (96 486C mol^{-1}), V is the bulk volume (L), I is the average current (A), and t is the time (s). C_0 and C_f denote the initial and final concentrations of bromate ions (mol L^{-1}). All experiments were conducted at room temperature (~20 °C).

Energy consumption (kW h mol^{-1}) was calculated using the following equation:

$$\mathrm{EC} = \frac{UIt}{(C_0 - C_f)\mathrm{V}} \tag{7}$$

where U was the applied cell voltage (V).

Results and discussion

Physical characterization

The sheet electrode and IREM were characterized using X-ray diffraction (XRD), as shown in Fig. 2. The XRD patterns confirmed that both electrodes primarily consisted of MP titanium oxide (Ti_4O_7), with a characteristic peak at 20.78°, along with a minor presence of Ti_6O_{11}, identified by its peak at 22.84°.[33] In addition to MP titanium oxide, a small fraction of potassium/titanium oxide was introduced during the heat sintering fabrication process to enhance the electrode's conductivity. The manufacturer incorporated this component into the membrane for improved electrical performance; however, the exact quantity was not disclosed and was not assessed in this study.

Magnéli phase titanium oxide sheet electrode

Fig. 3a presents the linear sweep voltammetry (LSV) (scan rate = 10 mV s^{-1}, background due to hydrogen evolution reaction (HER) subtracted (Fig. S1†)) of the sheet electrode in 100 mM KH_2PO_4 buffer with 1 mM, 5 mM, and 10 mM bromate ion concentrations. It could be observed that with increased bromate concentration, the cathodic current increased, which indicated bromate ions were indeed electro-reduced by the MP electrode. The onset of bromate reduction was observed at

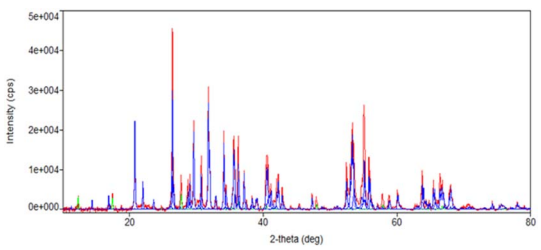

Fig. 2 XRD result of IREM material (red), standard of MP titanium oxide (blue), and standard of potassium titanium oxide (green). The sheet electrode was made of the same material.

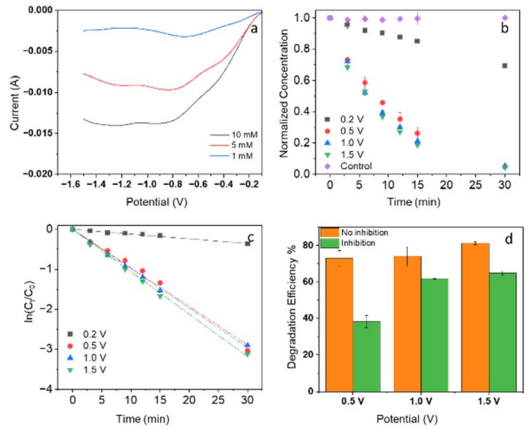

Fig. 3 (a) LSV analysis of bromate ions reduction with various concentrations at sheet electrode (100 mM KH_2PO_4), (b) effect of electrode potential (*vs.* Ag/AgCl) (c) kinetic pseudo-first-order rate at different electrode potential, and (d) effect of atomic hydrogen scavenger at −0.5, −1.0, and −1.5 V *vs.* Ag/AgCl. Concentrations are expressed relative to the measured initial concentration for each trial. Time is in minutes.

approximately −0.1 V *vs.* Ag/AgCl, indicating the initial electrochemical activity. The observed plateau current at −0.7 to −0.8 V suggests that the reaction may have been limited by mass transfer or surface site saturation rather than being kinetically controlled. If the reaction were kinetically limited, an increase in cathodic potential would have led to a further increase in current; however, the observed plateau indicates that mass transport constraints played a dominant role.

The electroreduction of bromate has been extensively studied using various electrode materials, including metallic electrodes (*e.g.*, Pt, Pd/In), metal/metal oxide-carbon composite electrodes (*e.g.*, Pd/rGO/CFP, Pd/GAC particles, graphene-modified Pd/C), modified carbon electrodes (*e.g.*, PANI/glassy carbon), and BDD.[40] Glasco *et al.* investigated bromate reduction on a Pt electrode using LSV, reporting an onset potential of −0.55 V *vs.* Ag/AgCl, a peak current around −1.0 V, and a sharp increase in current at −1.1 V due to the HER.[41] Other studies have highlighted the high HER overpotential associated with MP titanium oxide materials.[42]

In this study, bromate reduction on the sheet electrode initiated at approximately −0.1 V *vs.* Ag/AgCl, a significantly less negative potential than that reported for BDD (−0.45 V *vs.* SCE, in neutral solution)[25] On Pt, in strong acid, the reduction initiates at ∼+0.7 V SCE,[14] and in strong alkali at −0.55 V *vs.* Ag/AgCl.[41]

Effect of cathodic potentials on bromate removal

A control experiment without electrolysis was performed, confirming that no reduction in bromate concentration occurred in the electrochemical cell, as shown in Fig. 3b. This result indicates that the MP titanium oxide electrode did not induce a catalytic reduction of bromate ions without electrochemical polarization and that bromate adsorption on the electrode was negligible. Upon applying cathodic potentials to the sheet electrode, bromate reduction was observed with the concurrent formation of bromide ions. After 30 minutes of electrolysis, the measured total molar concentration of bromate and bromide ions was slightly lower than the initial bromate concentration (1 mM), within the experimental error (Fig. S2†). While this suggests minimal formation of stable intermediate species, the possibility of transient intermediates cannot be ruled out. Bromous acid ($HBrO_2$) and hypobromous acid (HOBr) have been reported as potential intermediates in previous studies; however, they are known to be unstable.[25,43]

The effect of cathodic potential on bromate reduction kinetics was investigated, as shown in Fig. 3b. Bromate reduction was observed at −0.2 V, consistent with the LSV results in Fig. 3a. At lower cathodic potentials, the bromate removal rate became independent of potential, indicating mass transfer limitations at the electrode, as evidenced by the current plateau in Fig. 3a. The highest current efficiency was achieved at −0.5 V (Table 1). As the cathodic potential increased, the background current also increased, while the diffusion-limited current for bromate electroreduction remained constant, leading to a decrease in current efficiency (CE). The rise in background current at potentials more negative than −0.5 V (Fig. S1†) could be attributed to the cathodic reduction of the electrode material or, more likely, the HER. The proton discharge associated with HER may also facilitate hydrogen insertion into the electrode material near the surface.

The calculated kinetic rate constants for bromate reduction are presented in Table 1. As shown in Fig. 3c, the reduction rate constant increased with increasing cathodic potential. The improvement in degradation efficiency (DE) was pronounced at lower potential biases (0 V to −0.5 V) but became marginal at higher biases (−0.5 V to −1.5 V), further supporting a diffusion-controlled bromate electroreduction process.

Bromate ions can be directly reduced *via* electron tunneling or through chemisorption complex formation with the cathode.[20,44] Another potential reduction mechanism involves the generation of surface-adsorbed atomic hydrogen (H*) on the cathode surface, a highly reactive intermediate. The production of H* typically requires transition metals (*e.g.*, Cu, Ni, Pd, Ag),[45] metal oxides (*e.g.*, WO_3),[46,47] or carbon-based materials (*e.g.*, graphene)[47,48] to facilitate hydrogen activation from water.[20,49–52] Recent studies have also reported the formation of atomic H* on MP Ti_4O_7.[29]

To investigate the role of H* in bromate reduction, tertiary butanol (TBA) was introduced as an atomic H* scavenger.[29,53,54] In this study, the addition of TBA resulted in a decrease in bromate degradation efficiency (Table 2), suggesting that

Table 1 Reduction of bromate ions with sheet electrode in 30 min

	Voltage			
	−0.2	−0.5	−1.0	−1.5
DE (%)	31	95	95	96
CE (%)	7.9	15	10	5.1
Kinetic rate constant (min^{-1})	0.012	0.097	0.099	0.106

Table 2 Inhibition effect by TBA in 15 min

	NO TBA			With TBA		
Voltage	−0.5	−1.0	−1.5	−0.5	−1.0	−1.5
DE/%	74	74	81	38	62	65

atomic H* plays a role in the bromate reduction process. However, as previously noted, MP Ti_4O_7 presents an intriguing possibility where atomic hydrogen, formed during water reduction, could also be incorporated into the electrode lattice at the surface, potentially contributing to bromate reduction.[38,55]

Effect of ion inhibition

Prior studies have demonstrated that the presence of interfering anions, such as SO_4^{2-}, Cl^-, SiO_3^{2-}, and CO_3^{2-}, can significantly suppress the electroreduction of bromate, leading to reduced bromate removal efficiency. The inhibitory effect increases with anion concentration, as observed in studies using BDD electrodes.[25] Among these anions, SO_4^{2-} exhibited the strongest inhibition, followed by Cl^-, while SiO_3^{2-} and CO_3^{2-} showed similar effects. Similar inhibition trends have also been reported for catalytic bromate reduction elsewhere.[56–58]

To assess the feasibility of bromate reduction under realistic treatment conditions, we investigated the influence of various coexisting anions (NO_3^-, NO_2^-, Cl^-, ClO_4^-, SO_4^{2-}, and CO_3^{2-}) by separately introducing them into the solution.

At a lower anion concentration of 1 mM, the inhibition effect was less pronounced (Fig. 4a). However, as shown in Fig. 4b, the inhibition increased at a concentration of 10 mM. The bromate reduction efficiencies at −1.0 V after 15 minutes were 46, 57, 62, 64, 66, 73, and 74% for solutions containing SO_4^{2-}, CO_3^{2-}, Cl^-, NO_3^-, NO_2^-, ClO_4^-, and no coexisting ion, respectively. The inhibition effect followed the order: $SO_4^{2-} > CO_3^{2-} > Cl^- \approx NO_3^- \approx NO_2^- > ClO_4^-$. A similar trend was observed at −1.5 V, although SO_4^{2-} and CO_3^{2-} exhibited nearly identical inhibition effects.

SO_4^{2-} exhibited the strongest inhibitory effect on bromate reduction, consistent with previous studies, of electroreduction on BDD or Pd, or of catalytic reduction by hydrogen, on Pd and Pt.[8,57,58] However, CO_3^{2-} demonstrated a strong inhibition effect at −1.0 V comparable to SO_4^{2-} at 1 mM anion concentrations, which contrasts with previous findings.[25] Competitive adsorption of the anions onto reactive surface sites has been suggested as the mechanism; that this might be dependent on the nature of the surface is not unexpected, particularly given the complexity of the reaction mechanism.

The inhibition effect may be explained by the competitive binding of active electrode sites by coexisting ions.[57] Additionally, the inhibition effect was relatively strong when SO_4^{2-}, CO_3^{2-}, or Cl^- was present. This may be due to the formation of strong oxidizing species at the anode in the undivided cell, such as peroxydisulfate ($S_2O_8^{2-}$), peroxodicarbonate ($C_2O_6^{2-}$), and chlorine-based oxidants (Cl_2, HOCl, ClO^-), which could potentially re-oxidize reaction intermediates back to bromate.[59]

The formation of these oxidants occurs *via* the following electrochemical reactions at the anode:

$$2SO_4^{2-} \rightarrow S_2O_8^{2-} + 2e^- \quad E^0 = 2.01 \text{ V } vs. \text{ SHE} \tag{8}$$

$$2CO_3^{2-} \rightarrow C_2O_6^{2-} + 2e^- \quad E^0 \approx 1.90 \text{ V } vs. \text{ SHE} \tag{9}$$

$$2Cl^- \rightarrow Cl_{2(aq)} + 2e^- \quad E^0 = 1.36 \text{ V } vs. \text{ SHE} \tag{10}$$

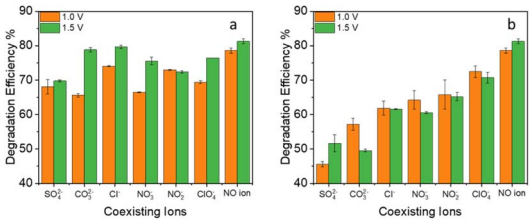

Fig. 4 (a) inhibition effect of 1 mM coexisting ions at −1.0 and −1.5 V, and (b) inhibition effect of 10 mM coexisting ions at −1.0 and −1.5 V. The experiments were conducted with an initial bromate concentration of 1 mM, and the degradation efficiency was calculated at 15 min.

Bromate under flow-through mode with IREM

Effect of cell potential. The cell potential is a critical factor in bromate reduction using IREM, as it influences not only degradation efficiency but also energy consumption and current efficiency, both of which are key considerations for the practical application of electrochemical treatment. In a study by Mao *et al.*, bromate degradation efficiencies were ~0%, 24%, and 87% at cathodic potentials of −0.5 V, −1.0 V, and −2.0 V, respectively. However, further increasing the cathodic potential to −2.5 V did not significantly enhance degradation efficiency.[3] Similarly, using a BDD electrode, the bromate reduction rate constant increased from 0.4 to 1.49 h^{-1} when the cathodic potential was increased from −0.3 V to −5.0 V.[25]

In this study, cell potentials of 2.5 V, 3.25 V, and 4.0 V were investigated, corresponding to cathodic potentials of approximately −1.01 V, −1.44 V, and −2.05 V *vs.* Ag/AgCl, respectively. As the applied cell potential increased, bromate degradation efficiency improved; however, this came at the expense of increased energy consumption, as shown in Table 3. The degradation kinetic rate also increased with increasing cell potential due to enhanced electron transport.[60] However, when the cell potential increased from 3.25 V to 4.0 V, the kinetic rate constant showed only a marginal increase, suggesting that the system reached a diffusion-limited regime. Moreover, the higher cathodic potential at 4.0 V likely promoted undesired side reactions, such as HER, leading to increased energy consumption and reduced efficiency.[61]

CE, which represents the proportion of charge utilized for bromate reduction, decreased with increasing cell potential, with values of 49%, 20%, and 15% for 2.5 V, 3.25 V, and 4.0 V, respectively. Whilst the CE at 3.25 V is lower than at 2.5 V, this cell potential was chosen as optimal between the three tested potentials because it provided a balance between DE, kinetic

Table 3 Degradation efficiency (DE), energy consumption (EC), current efficiency (CE), %, and kinetic rate are constant under different cell voltages and pH levels. The cell voltage was 3.25 V, and the pH was 6.89 if not mentioned otherwise

	Cell voltage (V)			pH		
Variable	2.5	3.25	4	11	2.49	6.89
DE (%)	15	99	98	95	99	100
EC (kW h mol^{-1})	0.83	1.8	4.4	2.9	2.7	2.6
CE (%)	49	20	15	18	19	20
Kinetic rate constant (min^{-1})	0.0017	0.043	0.038	0.029	0.056	0.051

rate, current efficiency, and energy consumption. Although 2.5 V exhibited the highest CE (49%), it resulted in a lower degradation rate, which is undesirable for practical applications. Conversely, 4.0 V showed a high but similar DE as 3.25 V but suffered from excessive energy consumption and low current efficiency (15%) due to increased side reactions. Therefore, 3.25 V was selected as the optimal condition, as it provided a compromise between efficiency and operational feasibility for subsequent experiments.

Effect of pH. In this study, the electrochemical reduction of bromate ions was influenced by the solution pH, as illustrated in Fig. 5b and Table 3. The final bromate degradation efficiencies at pH 11, pH 2.49, and near-neutral pH were 95%, 99%, and 99.7%, respectively. Although the fastest reduction (reaching >98% removal by 40 min) was observed under acidic conditions (pH 2.49), the overall difference in final efficiency between pH 2.49 and pH 11 was relatively small.

These findings align partially with previous studies. For instance, Mao *et al.* (2014) demonstrated a significant decrease in electroreduction rate (from 0.0203 to 0.0014 min^{-1}) as pH increased from 2.73 to 9.39 using a Pd-modified carbon fiber electrode.[3] Conversely, Lan *et al.* (2016) reported only a weak pH dependence for bromate reduction,[62] suggesting the influence of pH may vary depending on the electrode material and operational conditions.

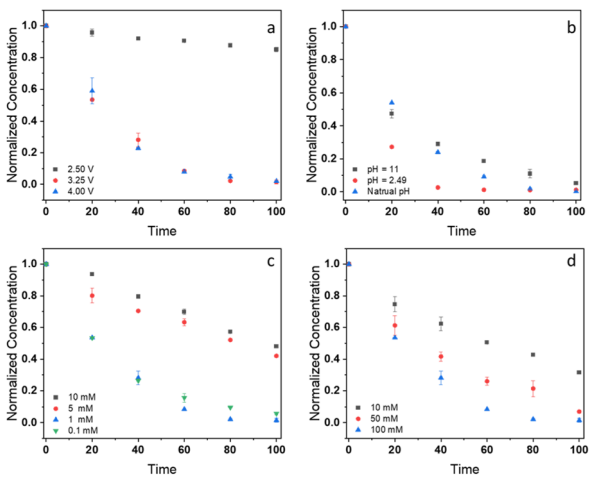

Fig. 5 Effect of (a) different cell voltage, (b) pH, (c) initial bromate concentration, and (d) electrolyte concentration ($NaClO_4$). Concentration is normalized to the initial concentration in the solution. Time is in minutes.

Kishimoto and Matsuda highlighted that lowering the solution pH can increase the current efficiency for bromate removal, possibly due to the shift in the chemical equilibrium of the bromate reduction reaction. However, they also noted that the dissociation constant (73.9 mol L^{-1}) for bromic acid ($HBrO_3$) is so high that under most experimental conditions, bromate remains predominantly in its ionic form.[13] Consequently, the notion that bromic acid ($HBrO_3$) is formed in large amounts at low pH is not strongly supported. Thus, the enhanced bromate reduction in acidic media may be better explained by (i) the increased availability of protons (H^+) for direct electroreduction (eqn (1) and (2)) and (ii) the formation of surface-adsorbed atomic hydrogen (H*) in the indirect pathway.[8,63]

In the indirect reduction pathway, protons from water can be reduced to H* (atomic hydrogen; likely inserted into the titanium oxide surface), *via* the Volmer reaction, which can then react with bromate:

Volmer reaction:

$$H_2O + e^- \rightarrow H^* + OH^- \quad (11)$$

Bromate reduction *via* H*:

$$BrO_3^- + 6H^* \rightarrow Br^- + 3H_2O \quad (12)$$

Thus, acidic conditions facilitate the generation of H^+ and, subsequently, H*, increasing the bromate reduction rate. Although the final removals at pH 2.49 and pH 11 were similar, the faster kinetics at low pH could be advantageous in practical scenarios where rapid bromate removal is desired, provided that managing acidic effluents is feasible. Research involving direct measurements of reaction intermediates (*e.g.*, $HBrO_2$ or atomic H*), could offer an enhanced understanding of the exact role of pH in bromate electroreduction.

Effect of initial bromate concentration. The initial reactant concentration plays a significant role in the electrochemical reduction process. To investigate its impact, experiments were conducted with initial bromate concentrations of 0.1, 1, 5, and 10 mM. As shown in Fig. 5c, at initial concentrations of 0.1 and 1 mM, bromate was nearly completely degraded within 100 min. However, as the initial bromate concentration increased to 5 and 10 mM, the degradation efficiency decreased to 58% and 52%, respectively. Although the overall removal efficiency declined at higher initial concentrations, the total amount of

bromate removed increased, indicating a higher absolute reduction capacity of the system.

The observed decrease in degradation efficiency at higher concentrations suggests that reaction kinetics rather than mass transfer limitations governed the process. While low bromate concentrations may be diffusion-limited, higher concentrations typically enhance mass transfer due to increased concentration gradients, promoting bromate transport to the electrode surface. Thus, the decline in degradation efficiency at 5 and 10 mM is more likely attributed to electrode surface saturation, competitive adsorption effects, or the formation of reaction intermediates rather than simple mass transfer limitations.

In contrast, energy consumption decreased significantly with increasing bromate concentration, with values of 27, 2.6, 1.3, and 0.93 kW h mol^{-1} for 0.1, 1, 5, and 10 mM, respectively. This trend is expected, as at higher concentrations, more bromate ions are available per unit charge, improving the utilization efficiency of the applied current.

Overall, while higher initial bromate concentrations resulted in lower removal efficiencies, they enhanced absolute bromate removal and significantly reduced energy consumption, which is an important consideration for practical applications. Future studies could explore strategies to mitigate possible electrode saturation or side reactions at elevated bromate concentrations to maintain high efficiency across a broader range of initial concentrations.

Effect of electrolyte concentration. Electrolyte concentration plays a crucial role in determining the conductivity of the solution, which in turn affects bromate degradation efficiency. In a study by Mao *et al.* (2014), increasing the electrolyte concentration from 0.1 mM to 10 mM significantly improved bromate degradation efficiency, reducing the treatment time from 120 min (25.5% removal) to just 30 min (almost 100% removal).[3]

In this study, since the cell potential was controlled, increasing the electrolyte concentration led to a decrease in bulk solution resistance and, consequently, a higher cathodic potential. This enhanced potential at the cathode accelerated both the direct and indirect electrochemical reduction of bromate, thereby improving degradation efficiency (Fig. 5d and Table 4).

However, while increased conductivity facilitated bromate reduction, it may also promote undesired side reactions, such as the HER and possible cathodic reduction of other species, leading to higher energy consumption (Table 4). This trade-off between enhanced bromate removal and increased energy demand highlights the need for optimized electrolyte concentrations to balance efficiency and energy costs in practical applications.

Bromate removal in the secondary effluent wastewater. The electroreduction of bromate was investigated in secondary effluent wastewater with an initial 1 mM bromate concentration (Fig. 6). The kinetic rate constant was 3.7×10^{-3} min^{-1} (Fig. 6b), which was much lower than that of 0.051 min^{-1} in synthetic solution (3.25 V, 100 mM $NaClO_4$).

This reduction in reaction rate can likely be attributed to two main factors: (a) lower conductivity – the conductivity of the secondary effluent was not directly measured in this study, but wastewater generally has lower ionic strength compared to synthetic 100 mM electrolyte solutions. A lower conductivity would increase solution resistance, potentially reducing the effective cathodic potential and slowing down the electroreduction process; and (b) the presence of organic and inorganic contaminants – secondary effluent contains a mixture of dissolved organic matter, inorganic anions, and residual nutrients, which can compete for active sites on the electrode surface. These species may also scavenge electrons or reactive intermediates, further reducing the efficiency of bromate reduction.

While the results indicate that electrochemical bromate reduction is feasible in real wastewater matrices, optimizing the process for practical applications will require addressing competitive effects from coexisting contaminants and potentially adjusting solution conductivity to improve efficiency.

Reusability

Reusability tests were conducted for both the MP titanium oxide sheet electrode and IREM, with each cycle lasting 30 min for the

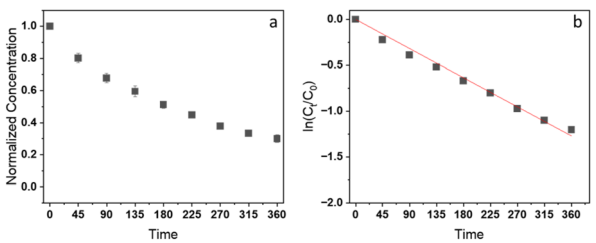

Fig. 6 (a) Removal of bromate in secondary effluent, and (b) linear fitting for the kinetic rate constant. Time is in minutes.

Table 4 Degradation efficiency, energy consumption, current efficiency, and kinetic rate constant under different initial bromate concentrations and electrolyte concentrations. The cell potential was 3.25 V, pH was 6.89, and initial bromate concentration was 1 mM, if not mentioned otherwise

	Initial bromate concentration (mM)				Electrolyte concentration (mM)		
Variable	0.1	1	5	10	10	50	100
DE (%)	94	99	58	52	68	93	99
EC (kW h mol^{-1})	27	2.6	1.3	0.9	0.9	1.3	2.6
CE (%)	2	20	40	56	57	40	20
Kinetic rate constant (min^{-1})	0.030	0.043	0.008	0.007	0.011	0.024	0.043

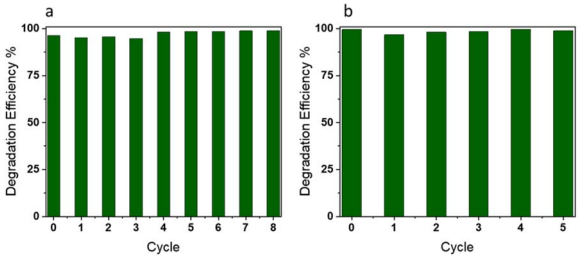

Fig. 7 Reusability of (a) sheet electrode and (b) IREM.

sheet electrode and 100 min for the IREM. Even after 7 cycles (sheet electrode) and 5 cycles (IREM) without intermediate cleaning, both electrodes maintained a high bromate degradation rate (Fig. 7). The sustained performance over multiple cycles highlights the stability and durability of MP titanium oxide, demonstrating its promising potential for real-world water and wastewater treatment applications.

Conclusions

This study investigated bromate reduction using MP titanium oxide sheet electrodes and IREM, demonstrating their promising potential for water and wastewater treatment applications. However, the mechanism of bromate reduction may differ between the two systems. According to Vorotyntsev *et al.* (2019), in flow-through porous electrodes (IREM), the reduction of non-electroactive species like bromate may involve an autocatalytic process mediated by Br_2/Br^- species. In this mechanism, Br_2/Br^- is initially generated on the electrode surface, followed by a comproportionation reaction between bromate and Br^-, regenerating Br_2.[15] These findings suggest that optimizing the length-to-flow velocity ratio in IREM channels could further enhance bromate removal efficiency.

While sodium perchlorate was used as an inert electrolyte in this study, previous research has shown that perchlorate can be electrochemically reduced under certain conditions.[64–66] Although Almassi *et al.* (2022) confirmed that perchlorate remains stable between −0.4 to −1.3 V *vs.* SHE on MP titanium oxide electrodes,[67] one experiment in this study was conducted at approximately −2.05 V *vs.* Ag/AgCl, where perchlorate reduction could potentially occur. Future research should evaluate the impact of perchlorate reduction on bromate degradation to confirm the reliability of this electrolyte for similar applications.

In summary, this study provides a comprehensive performance analysis of MP titanium oxide electrodes for bromate reduction, considering the influence of experimental conditions and coexisting ions. MP titanium oxide offers a stable, efficient, and potentially cost-effective solution for bromate removal from water. Future studies should focus on optimizing operational parameters and exploring long-term electrode performance in real-world applications.

Data availability

Additional supporting data is provided in the ESI accompanying this article.†

Author contributions

LG: experimental design, conducting experiments, data acquisition, and analysis, literature review, writing the original manuscript; DEW: reviewed and revised the manuscript, cosupervision; LB: reviewed and revised the manuscript; LPP: experimental design, funding acquisition, reviewed and revised the manuscript, supervision.

Conflicts of interest

There are no conflicts of interest to declare.

Acknowledgements

LG acknowledges lab technical staff at the University of Auckland, Dr Patricia Cabedo Sanz, Dr Meet Mistry, Dr Jishan Liu, and Dr Yantao Song, for their help with the analysis. LG would also like to thank Gary Brant, Senior Technician at the University of Auckland, for his help in the design and manufacture of the electrochemical reactor.

References

1 R. A. Y. Butler, A. Godley, L. Lytton and E. Cartmell, Bromate Environmental Contamination: Review of Impact and Possible Treatment, *Crit. Rev. Environ. Sci. Technol.*, 2005, **35**(3), 193–217.
2 S. W. Krasner, W. H. Glaze, H. S. Weinberg, P. Daniel and I. N. Najm, Formation and control of bromate during ozonation of waters containing bromide, *J.–Am. Water Works Assoc.*, 1993, **85**, 73–81.
3 R. Mao, X. Zhao and J. Qu, Electrochemical reduction of bromate by a Pd modified carbon fiber electrode: kinetics and mechanism, *Electrochim. Acta*, 2014, **132**, 151–157.
4 U. v. Gunten, Ozonation of drinking water: Part II. Disinfection and by-product formation in presence of bromide, iodide or chlorine, *Water Res.*, 2003, **37**, 1469–1487.
5 S. Hong, S. Deng, X. Yao, B. Wang, Y. Wang, J. Huang and G. Yu, Bromate removal from water by polypyrrole tailored activated carbon, *J. Colloid Interface Sci.*, 2016, **467**, 10–16.
6 A. N. Davidson, J. Chee-Sanford, H. Y. Lai, C. H. Ho, J. B. Klenzendorf and M. J. Kirisits, Characterization of bromate-reducing bacterial isolates and their potential for drinking water treatment, *Water Res.*, 2011, **45**(18), 6051–6062.
7 J. Restivo, O. S. G. P. Soares, J. J. M. Órfão and M. F. R. Pereira, Metal assessment for the catalytic reduction of bromate in water under hydrogen, *Chem. Eng. J.*, 2015, **263**, 119–126.
8 H. Chen, Z. Xu, H. Wan, J. Zheng, D. Yin and S. Zheng, Aqueous bromate reduction by catalytic hydrogenation over Pd/Al2O3 catalysts, *Appl. Catal., B*, 2010, **96**(3–4), 307–313.
9 F. Chen, Q. Yang, Y. Zhong, H. An, J. Zhao, T. Xie, Q. Xu, X. Li, D. Wang and G. Zeng, Photo-reduction of bromate in drinking water by metallic Ag and reduced graphene oxide

(RGO) jointly modified BiVO4 under visible light irradiation, *Water Res.*, 2016, **101**, 555–563.

10 Q. Xiao, S. Yu, L. Li, Y. Zhang and P. Yi, Degradation of bromate by Fe(II)Ti(IV) layered double hydroxides nanoparticles under ultraviolet light, *Water Res.*, 2019, **150**, 310–320.

11 C. T. Matos, S. Velizarov, M. A. M. Reis and J. G. Crespo, Removal of bromate from drinking water using the ion exchange membrane bioreactor concept, *Environ. Sci. Technol.*, 2008, **42**, 7702–7708.

12 A. Bard, R. Parsons, and J. Jordan, *Standard Potentials in Aqueous Solution*, CRC Press, 1985.

13 N. Kishimoto and N. Matsuda, Bromate ion removal by electrochemical reduction using an activated carbon felt electrode, *Environ. Sci. Technol.*, 2009, **43**(6), 2054–2059.

14 G. E. Badea and B. Teodora, Kinetics and mechanism of the bromate electrochemical reduction at platinum electrode, *Rev. Roum. Chim.*, 2006, **51**, 127–133.

15 M. A. Vorotyntsev and A. E. Antipov, Bromate electroreduction in acidic solution inside rectangular channel under flow-through porous electrode conditions, *Electrochim. Acta*, 2019, **323**, 134799.

16 W. Shen, F. Lin, X. Jiang, H. Li, Z. Ai and L. Zhang, Efficient removal of bromate with core-shell Fe@Fe2O3 nanowires, *Chem. Eng. J.*, 2017, **308**, 880–888.

17 C. Fan, N. Chen, C. Feng, Y. Yang, J. Qin, M. Li and Y. Gao, Enhanced performance and mechanism of bromate removal in aqueous solution by ruthenium oxide modified biochar (RuO2/BC), *Colloids Surf., A*, 2019, **572**, 27–36.

18 J. Restivo, O. S. G. P. Soares, J. J. M. Órfão and M. F. R. Pereira, Catalytic reduction of bromate over monometallic catalysts on different powder and structured supports, *Chem. Eng. J.*, 2017, **309**, 197–205.

19 Q. Li, Q. Zhang, L. Ding, D. Zhou, H. Cui, Z. Wei and J. Zhai, Synthesis of silver/multi-walled carbon nanotubes composite and its application for electrocatalytic reduction of bromate, *Chem. Eng. J.*, 2013, **217**, 28–33.

20 R. Mao, X. Zhao, H. Lan, H. Liu and J. Qu, Efficient electrochemical reduction of bromate by a Pd/rGO/CFP electrode with low applied potentials, *Appl. Catal., B*, 2014, **160–161**, 179–187.

21 E. Marafon, L. T. Kubota and Y. Gushikem, FAD-modified SiO2/ZrO2/C ceramic electrode for electrocatalytic reduction of bromate and iodate, *J. Solid State Electrochem.*, 2008, **13**(3), 377–383.

22 R. Mao, X. Zhao, H. Lan, H. Liu and J. Qu, Graphene-modified Pd/C cathode and Pd/GAC particles for enhanced electrocatalytic removal of bromate in a continuous three-dimensional electrochemical reactor, *Water Res.*, 2015, **77**, 1–12.

23 L. Ding, Q. Li, H. Cui, R. Tang, H. Xu, X. Xie and J. Zhai, Electrocatalytic reduction of bromate ion using a polyaniline-modified electrode: An efficient and green technology for the removal of BrO3− in aqueous solutions, *Electrochim. Acta*, 2010, **55**(28), 8471–8475.

24 L. Ding, Q. Li, D. Zhou, H. Cui, H. An and J. Zhai, Modification of glassy carbon electrode with polyaniline/multi-walled carbon nanotubes composite: Application to electro-reduction of bromate, *J. Electroanal. Chem.*, 2012, **668**, 44–50.

25 X. Zhao, H. Liu, A. Li, Y. Shen and J. Qu, Bromate removal by electrochemical reduction at boron-doped diamond electrode, *Electrochim. Acta*, 2012, **62**, 181–184.

26 I. G. Casella and M. Contursi, Electrochemical and spectroscopic characterization of a tungsten electrode as a sensitive amperometric sensor of small inorganic ions, *Electrochim. Acta*, 2005, **50**(20), 4146–4154.

27 S. O. Ganiyu, E. D. van Hullebusch, M. Cretin, G. Esposito and M. A. Oturan, Coupling of membrane filtration and advanced oxidation processes for removal of pharmaceutical residues: A critical review, *Sep. Purif. Technol.*, 2015, **156**, 891–914.

28 L. Guo, Y. Jing and B. P. Chaplin, Development and Characterization of Ultrafiltration TiO2 Magneli Phase Reactive Electrochemical Membranes, *Environ. Sci. Technol.*, 2016, **50**(3), 1428–1436.

29 C. Li, J. Zhu, Z. Zhao, J. Wang, Q. Yang, H. Sun and B. Jiang, An efficient and robust flow-through electrochemical Ti4O7 membrane system for simultaneous Cr (VI) reduction and Cr immobilization with membrane cleaning by a periodic polarity reversal strategy, *Sep. Purif. Technol.*, 2022, 121424.

30 C. Comninellis, Electrocatalysis in the electrochemical conversion/combustion of organic pollutants for waste water treatment, *Electrochim. Acta*, 1994, **39**, 1857–1862.

31 D. Huang, K. Wang, J. Niu, C. Chu, S. Weon, Q. Zhu, J. Lu, E. Stavitski and J.-H. Kim, Amorphous Pd-loaded Ti4O7 electrode for direct anodic destruction of perfluorooctanoic acid, *Environ. Sci. Technol.*, 2020, **54**(17), 10954–10963.

32 S. You, B. Liu, Y. Gao, Y. Wang, C. Y. Tang, Y. Huang and N. Ren, Monolithic porous Magnéli-phase Ti4O7 for electro-oxidation treatment of industrial wastewater, *Electrochim. Acta*, 2016, **214**, 326–335.

33 L. Guo, Y. Jing and B. P. Chaplin, Development and characterization of ultrafiltration TiO2 Magnéli phase reactive electrochemical membranes, *Environ. Sci. Technol.*, 2016, **50**(3), 1428–1436.

34 J. Zhang, Y. Zhou, B. Yao, J. Yang and D. Zhi, Current progress in electrochemical anodic-oxidation of pharmaceuticals: Mechanisms, influencing factors, and new technique, *J. Hazard. Mater.*, 2021, **418**, 126313.

35 S. Almassi, Z. Li, W. Xu, C. Pu, T. Zeng and B. P. Chaplin, Simultaneous Adsorption and Electrochemical Reduction of N-Nitrosodimethylamine Using Carbon-Ti4O7 Composite Reactive Electrochemical Membranes, *Environ. Sci. Technol.*, 2019, **53**(2), 928–937.

36 X. Cao, Z. Sun, X. Zheng, J. Tian, C. Jin, R. Yang, F. Li, P. He and H. Zhou, $MnCo_2O_4$ decorated Magnéli phase titanium oxide as a carbonfree cathode for Li-O_2 batteries, *J. Mater. Chem. A*, 2017, **37**(5), 19991–19996.

37 C. Trellu, B. P. Chaplin, C. Coetsier, R. Esmilaire, S. Cerneaux, C. Causserand and M. Cretin, Electro-oxidation of organic pollutants by reactive electrochemical membranes, *Chemosphere*, 2018, **208**, 159–175.

38 Y. JIng, Mechanistic study of electrochemical processes on a porous magnéli phase electrode, PhD thesis, University of Illinois, 2017.
39 B. P. Chaplin, Critical review of electrochemical advanced oxidation processes for water treatment applications, *Environ. Sci.:Processes Impacts*, 2014, **16**(6), 1182–1203.
40 E. Mousset and K. Doudrick, A review of electrochemical reduction processes to treat oxidized contaminants in water, *Curr. Opin. Electrochem.*, 2020, **22**, 221–227.
41 D. L. Glasco, A. Sheelam and J. G. Bell, Complex Dynamic Behavior During the Electro-Reduction of Bromate Ions, *J. Electrochem. Soc.*, 2022, **169**(5), 056509.
42 R. Pollock, J. Houlihan, A. Bain and B. Coryea, Electrochemical properties of a new electrode material, Ti4O7, *Mater. Res. Bull.*, 1984, **19**(1), 17–24.
43 C. Lee and M. Lister, The decomposition of aqueous sodium bromite, *Can. J. Chem.*, 1971, **49**(17), 2822–2826.
44 T. Li and J. Farrell, Reductive dechlorination of trichloroethene and carbon tetrachloride using iron and palladized-iron cathodes, *Environ. Sci. Technol.*, 2000, **34**(1), 173–179.
45 J. Deng, E. Gao, F. Wu, Z. You, X. Li, S. Gao and L.-Z. Huang, Generation of atomic hydrogen by Ni-Fe hydroxides: Mechanism and activity for hydrodechlorination of trichloroethylene, *Water Res.*, 2021, **207**, 117802.
46 Y. H. Li, P. F. Liu, L. F. Pan, H. F. Wang, Z. Z. Yang, L. R. Zheng, P. Hu, H. J. Zhao, L. Gu and H. G. Yang, Local atomic structure modulations activate metal oxide as electrocatalyst for hydrogen evolution in acidic water, *Nat. Commun.*, 2015, **6**(1), 1–7.
47 W. Zheng, Y. Liu, F. Liu, Y. Wang, N. Ren and S. You, Atomic Hydrogen in Electrocatalytic Systems: Generation, Identification, and Environmental Applications, *Water Res.*, 2022, 118994.
48 R. Mao, N. Li, H. Lan, X. Zhao, H. Liu, J. Qu and M. Sun, Dechlorination of trichloroacetic acid using a noble metal-free graphene–Cu foam electrode *via* direct cathodic reduction and atomic H, *Environ. Sci. Technol.*, 2016, **50**(7), 3829–3837.
49 J. Lipkowski and P. Ross, *Electrocatalysis*, Wiley-VCH Publishers, New York, 1998.
50 J. Radjenović, M. J. Farré, Y. Mu, W. Gernjak and J. Keller, Reductive electrochemical remediation of emerging and regulated disinfection byproducts, *Water Res.*, 2012, **46**(6), 1705–1714.
51 L. E. Knitt, J. R. Shapley and T. J. Strathmann, Rapid metal-catalyzed hydrodehalogenation of iodinated X-ray contrast media, *Environ. Sci. Technol.*, 2008, **42**(2), 577–583.
52 D. Shuai, B. P. Chaplin, J. R. Shapley, N. P. Menendez, D. C. McCalman, W. F. Schneider and C. J. Werth, Enhancement of oxyanion and diatrizoate reduction kinetics using selected azo dyes on Pd-based catalysts, *Environ. Sci. Technol.*, 2010, **44**(5), 1773–1779.
53 Q. Ji, D. Yu, G. Zhang, H. Lan, H. Liu and J. Qu, Microfluidic flow through polyaniline supported by lamellar-structured graphene for mass-transfer-enhanced electrocatalytic reduction of hexavalent chromium, *Environ. Sci. Technol.*, 2015, **49**(22), 13534–13541.
54 F. Ahmed, B. S. Lalia, V. Kochkodan, N. Hilal and R. Hashaikeh, Electrically conductive polymeric membranes for fouling prevention and detection: A review, *Desalination*, 2016, **391**, 1–15.
55 S. Fleischmann, Y. Sun, N. C. Osti, R. Wang, E. Mamontov, D.-e. Jiang and V. Augustyn, Interlayer separation in hydrogen titanates enables electrochemical proton intercalation, *J. Mater. Chem. A*, 2020, **8**(1), 412–421.
56 R. P. Pandey, K. Rasool, P. Abdul Rasheed and K. A. Mahmoud, Reductive sequestration of toxic bromate from drinking water using lamellar two-dimensional Ti3C2TX (MXene), *ACS Sustain. Chem. Eng.*, 2018, **6**(6), 7910–7917.
57 Z. Zhang, Y. Luo, Y. Guo, W. Shi, W. Wang, B. Zhang, R. Zhang, X. Bao, S. Wu and F. Cui, Pd and Pt nanoparticles supported on the mesoporous silica molecular sieve SBA-15 with enhanced activity and stability in catalytic bromate reduction, *Chem. Eng. J.*, 2018, **344**, 114–123.
58 Q. Xiao and S. Yu, Reduction of bromate from drinking water by sulfite/ferric ion systems: Efficacy and mechanisms, *J. Hazard. Mater.*, 2021, **418**, 125940.
59 J. Wang and L. Xu, Advanced oxidation processes for wastewater treatment: formation of hydroxyl radical and application, *Environ. Sci. Technol.*, 2012, **42**, 251–325.
60 X. H. Mao, A. Ciblak, M. Amiri and A. N. Alshawabkeh, Redox control for electrochemical dechlorination of trichloroethylene in bicarbonate aqueous media, *Environ. Sci. Technol.*, 2011, **45**, 6517–6523.
61 Y. Zhang, J. Ding, Q. Gao, B. Jiang, C. Li and Q. Zhao, Synthesis of low-cost Ti4O7 membrane electrode for electrooxidation of tetracycline under flow-through conditions: Performance, kinetics and mechanism, *Process Saf. Environ. Prot.*, 2022, **159**, 931–943.
62 H. Lan, R. Mao, Y. Tong, Y. Liu, H. Liu, X. An and R. Liu, Enhanced electroreductive removal of bromate by a supported Pd–In Bimetallic catalyst: kinetics and mechanism investigation, *Environ. Sci. Technol.*, 2016, **50**(21), 11872–11878.
63 M. R. Gennero de Chialvo and C. C. A, Kinetics of hydrogen evolution reaction with Frumkin adsorption: re-examination of the Volmer-heyrovsky and Volmer-tafel routes, *Electrochim. Acta*, 1998, **44**(5), 841–851.
64 C. Almeida, B. Giannetti and T. Rabockai, Electrochemical study of perchlorate reduction at tin electrodes, *J. Electroanal. Chem.*, 1997, **422**(1–2), 185–189.
65 M. Y. Rusanova, P. Polášková, M. Muzikař and W. R. Fawcett, Electrochemical reduction of perchlorate ions on platinum-activated nickel, *Electrochim. Acta*, 2006, **51**(15), 3097–3101.
66 L. Ye, H. You, J. Yao and H. Su, Water treatment technologies for perchlorate: a review, *Desalination*, 2012, **298**, 1–12.
67 S. Almassi, C. Ren, J. Liu and B. P. Chaplin, Electrocatalytic Perchlorate Reduction Using an Oxorhenium Complex Supported on a Ti4O7 Reactive Electrochemical Membrane, *Environ. Sci. Technol.*, 2022, **56**(5), 3267–3276.